Episodic activity in radio galaxies

D.J. Saikia

National Centre for Radio Astrophysics, TIFR, India

Collaborators

Chiranjib Konar, NCRA, TIFR, India
Marek Jamrozy, Uniwersytet Jagielloński, Poland
Jerzy Machalski, Uniwersytet Jagielloński, Poland
Neeraj Gupta, NCRA, TIFR, India
Ł. Stawarz, Uniwersytet Jagielloński, Poland
K.-H. Mack, Istituto di Radioastronomia, Italy
A. Siemiginowska, Harvard-Smithsonian Center for Astrophysics, USA

Introduction

Duration of their active galactic nuclei (AGN) phase?

Are such periods of activity episodic?

Radio loud and radio quiet dichotomy?

For radio loud objects history may be probed via structural and spectral information on the lobes of radio emission.

Double-double radio galaxies (DDRGs): a striking example of episodic jet activity.

Some results on episodic activity in radio galaxies using the Giant Metrewave Radio Telescope (GMRT) and the Very Large Array (VLA).

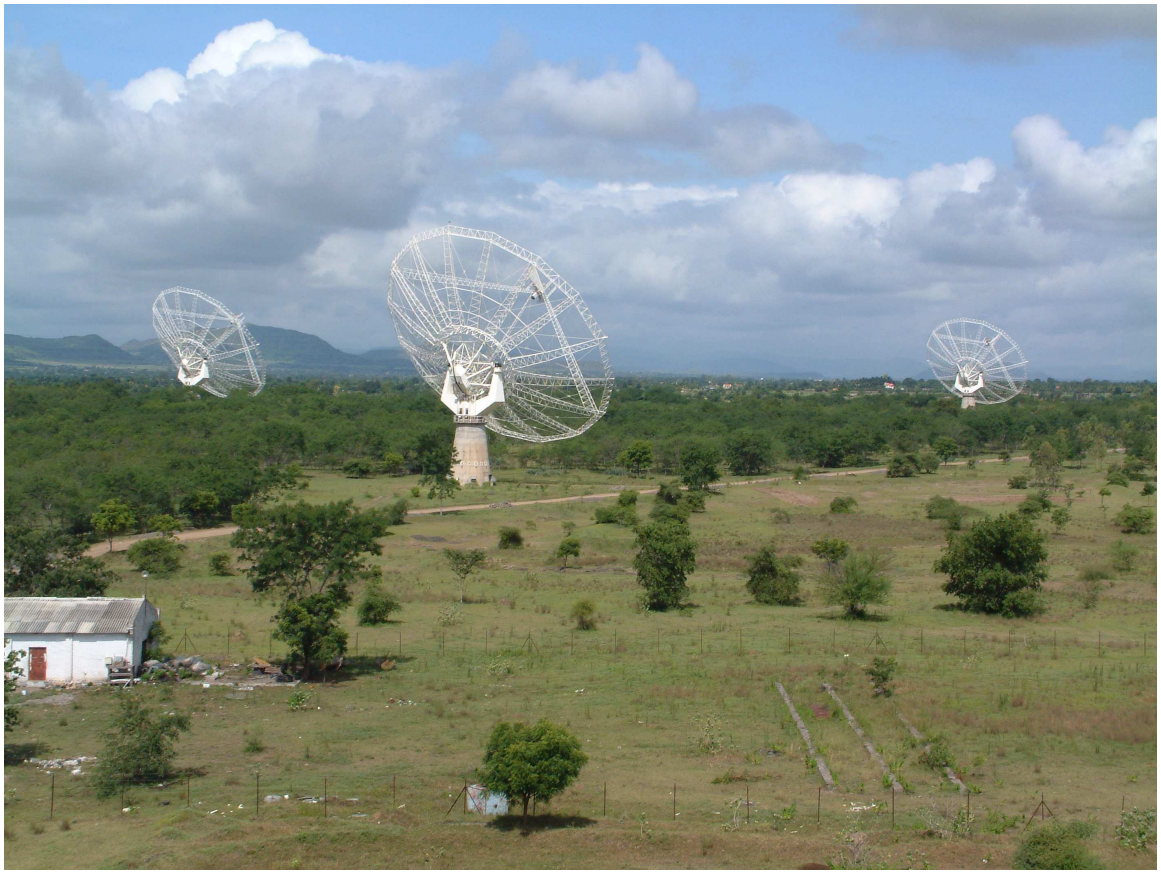

Figure 1: A view of three of the Central Square antennas of GMRT.

- **Thirty antennas each of 45 metre diameter, spread over ∼25 km**
- **Frequencies of operation: ∼150 MHz to 1400 MHz**
- **Angular resolution:**
  ∼20 arcsec (150 MHz) to 2 arcsec (1400 MHz)
- **rms sensitivities:**
  1.5 mJy beam^{-1} (150 MHz), 0.6 mJy beam^{-1} (235 MHz),
  0.3 mJy beam^{-1} (325 MHz), 0.02 mJy beam^{-1} (610 MHz),
  0.03 mJy beam^{-1} (1400 MHz)

J0041+3224: a new double-double radio galaxy discovered with the GMRT

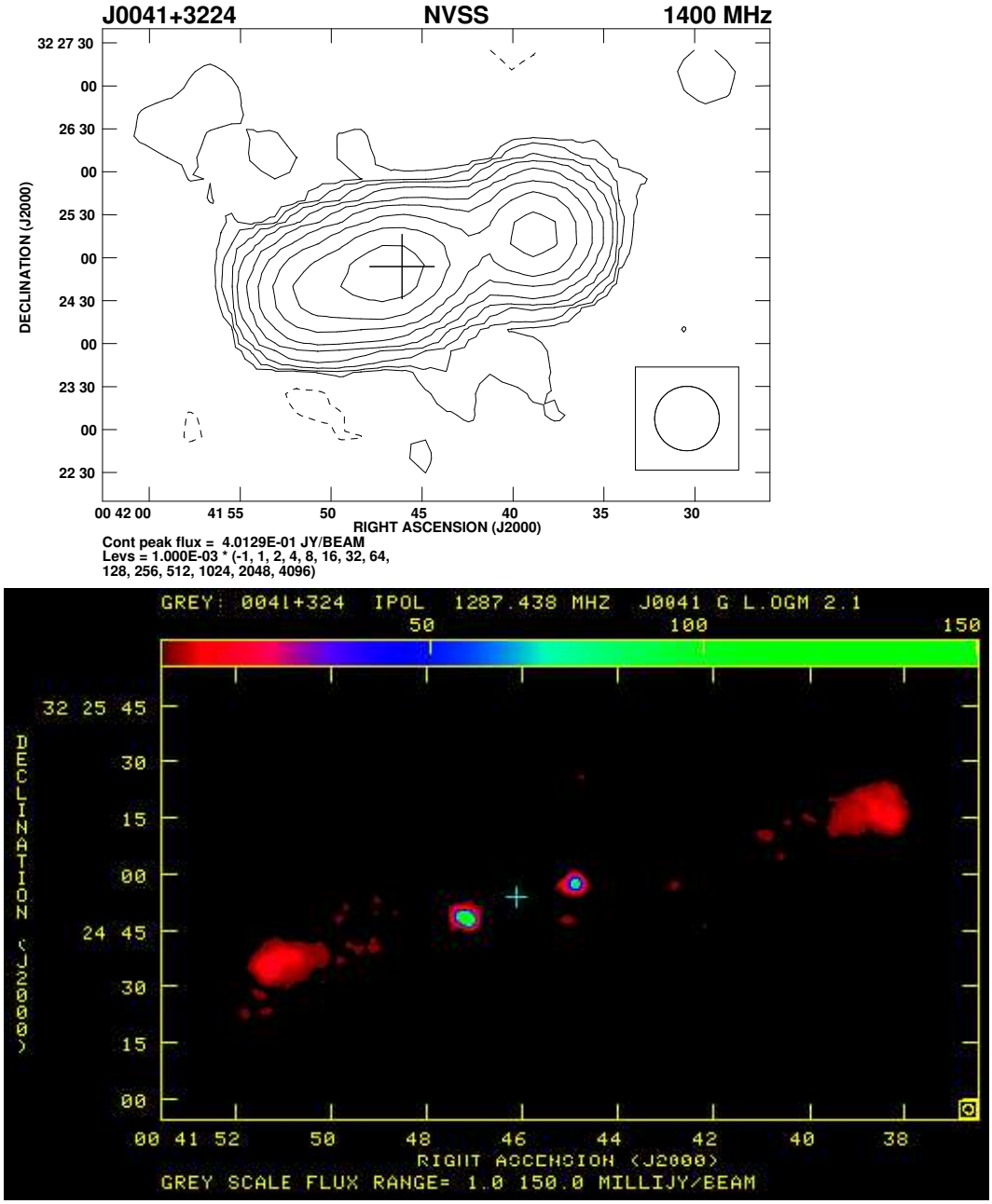

Figure 2: The NVSS image of J0041+3224 with an angular resolution of 45 arcsec (upper panel) and the GMRT image at 1287 MHz with an angular resolution of ∼2.7 arcsec (Saikia, Konar & Kulkarni 2006).

- **Outer size: 969 kpc; inner size: 171 kpc (estimated redshift = 0.45)**
- **Outer and inner luminosity: $\sim 3.3 \times 10^{26}$ W Hz^{-1} at 1400 MHz**

Spectra of the different components of J0041+3224

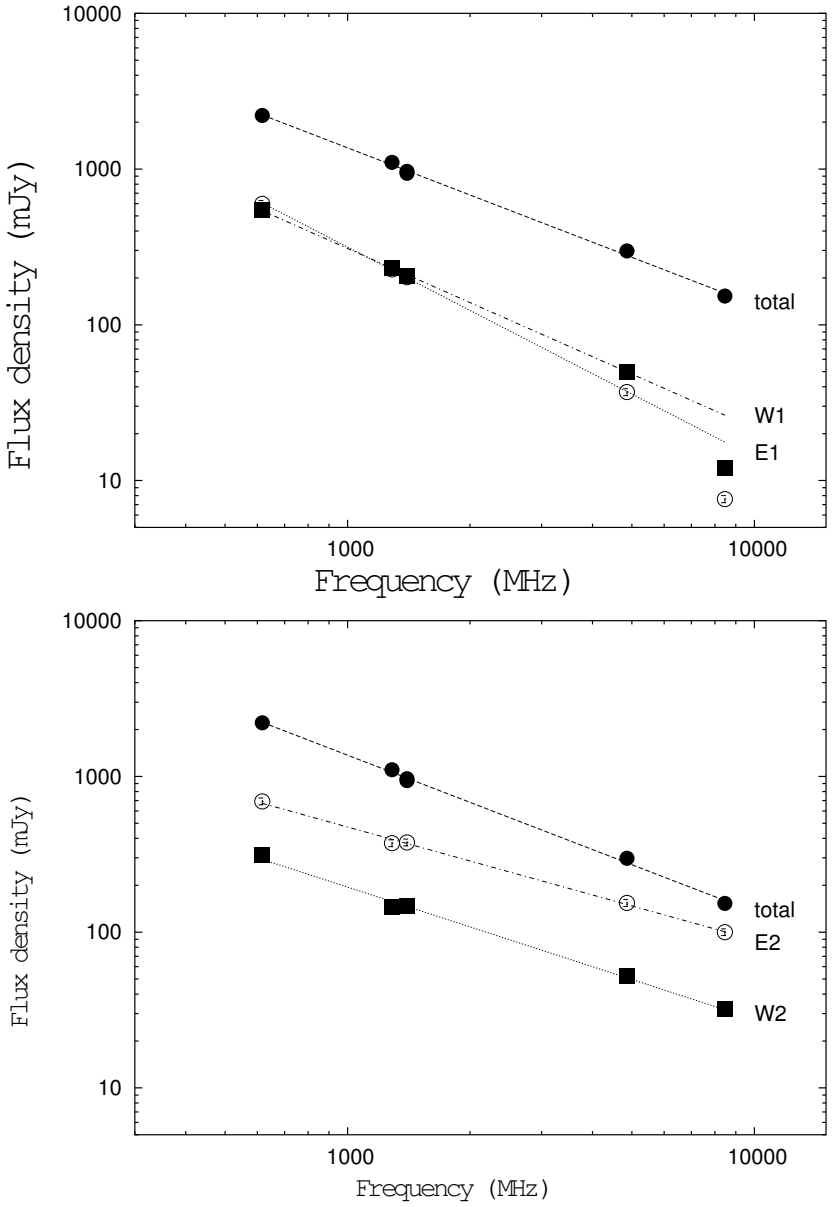

Figure 3: The spectra of the western and eastern components of the outer double (upper panel) and the inner double (lower panel). The integrated spectrum is shown in both the panels.

- **Spectral index of entire source: -1.01 ± 0.02 ($S\propto \nu^{\alpha}$)**
- **Spectral index of outer double: -1.15 ± 0.01 (western) and -1.35 ± 0.01 (eastern)**
- **Spectral index of inner double: -0.85 ± 0.03 (western) and -0.73 ± 0.02 (eastern)**

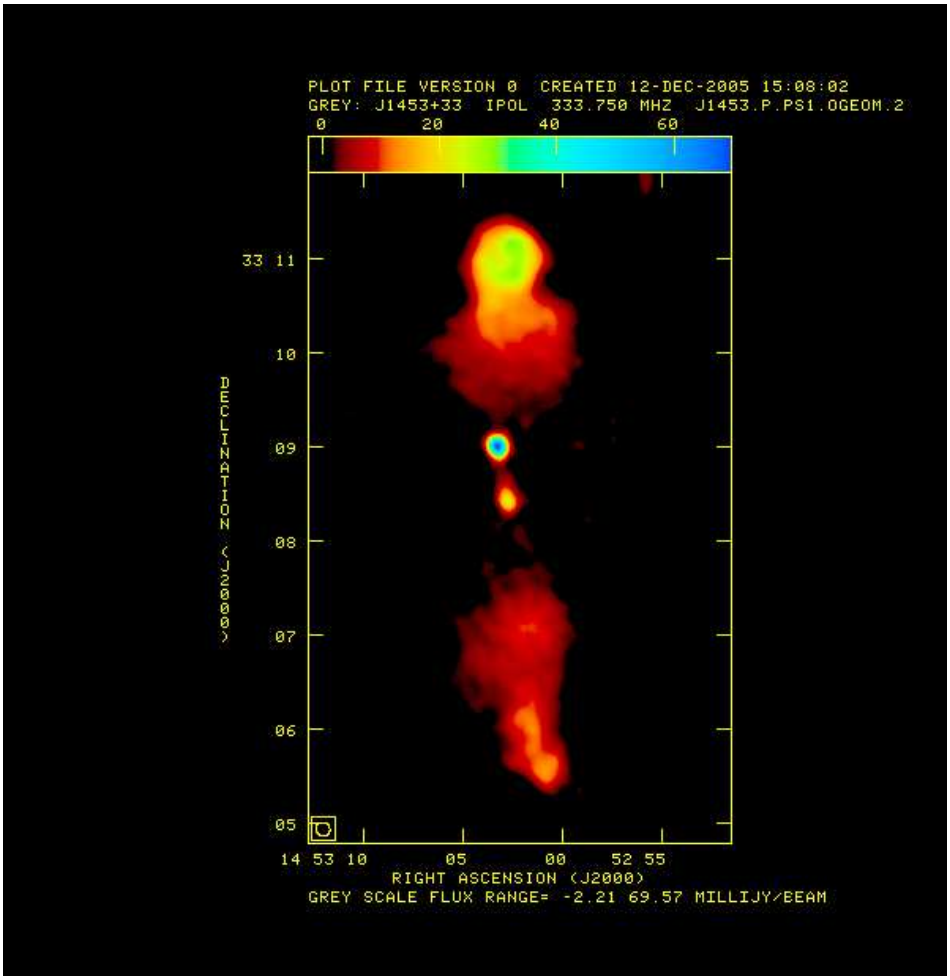

Figure 4: GMRT image of the double-double radio galaxy J1453+3308 at 334 MHz with a resolution of ∼9 arcsec (Konar, Saikia, Jamrozy & Machalski 2006).

- **Outer size: 1297 kpc; inner size: 159 kpc (redshift = 0.249)**
- **Outer luminosity: $\sim 7.9\times10^{25}$ W Hz^{-1} at 1400 MHz; inner luminosity: $\sim 5.9\times10^{24}$ W Hz^{-1} at 1400 MHz**

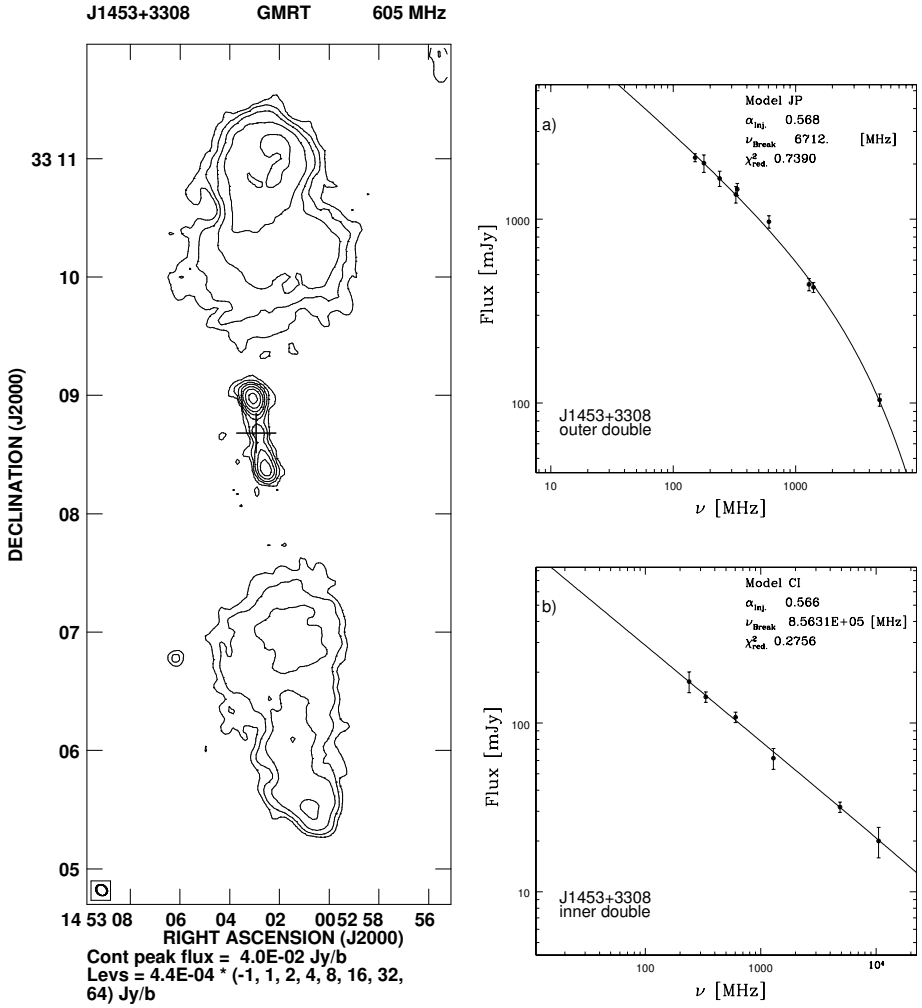

Figure 5: The GMRT image of the DDRG J1453+3308 at 605 MHz with an angular resolution of ∼5.4 arcsec. Spectra of the outer and inner doubles fitted with the models of radiative losses. Upper panel: the outer double fitted with the Jaffe-Perola model; lower panel: the inner double fitted with the continuous-injection model. (Konar, Saikia, Jamrozy & Machalski 2006).

- **Outer double: injection spectrum ∼0.57; break frequency ∼6700 MHz**
- **inner double: injection spectrum ∼0.57; break frequency ∼8.6×10^5 MHz**

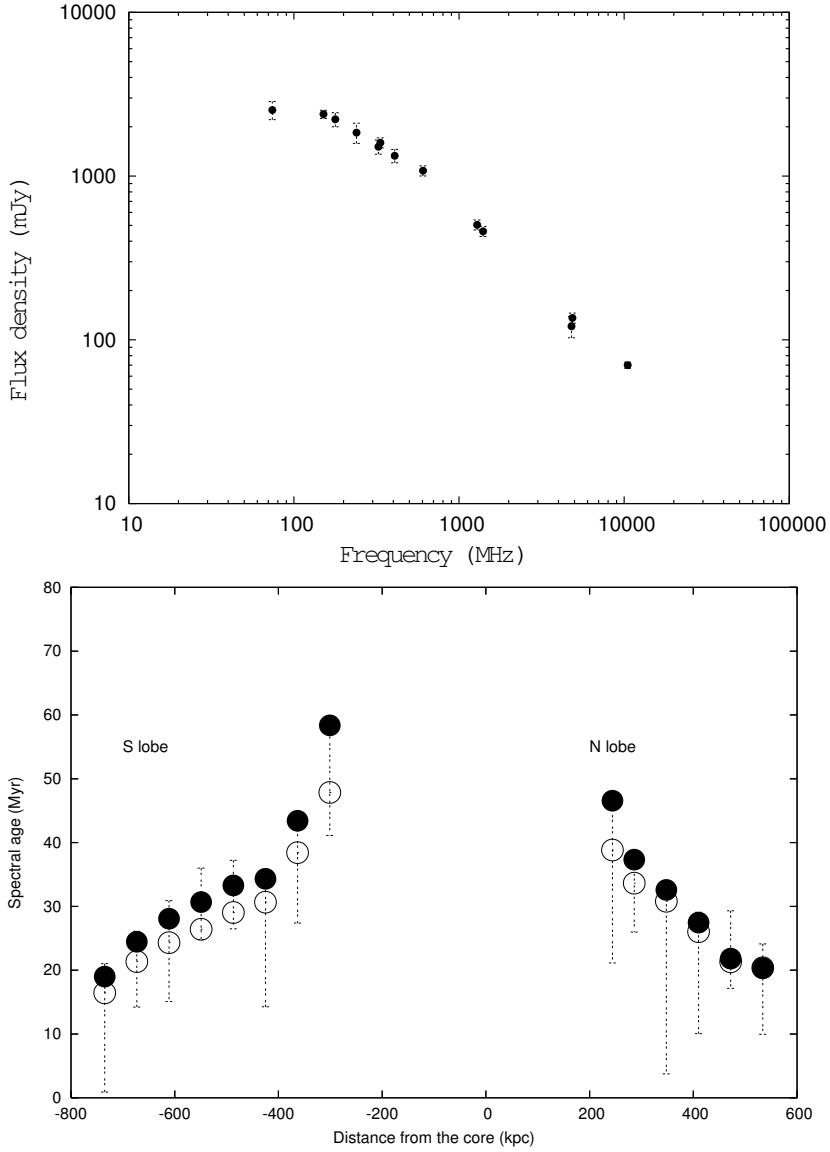

Figure 6: Radiative age of the relativistic particles in the outer lobes of J1453+3308 plotted against the distance from the radio core using the revised (filled circles) and classical (open circles) equipartition magnetic fields.

- **Maximum ages for the outer double: ∼47 Myr (northern) and ∼58 Myr (southern)**
- **Mean separation velocity of lobe head: ∼0.036c; maximum age: ∼ 134 Myr**
- **Spectral age of inner double: ∼2 Myr; apparent advance speed: ∼0.1c**
- **Variable core**

Symmetry parameters of DDRGs

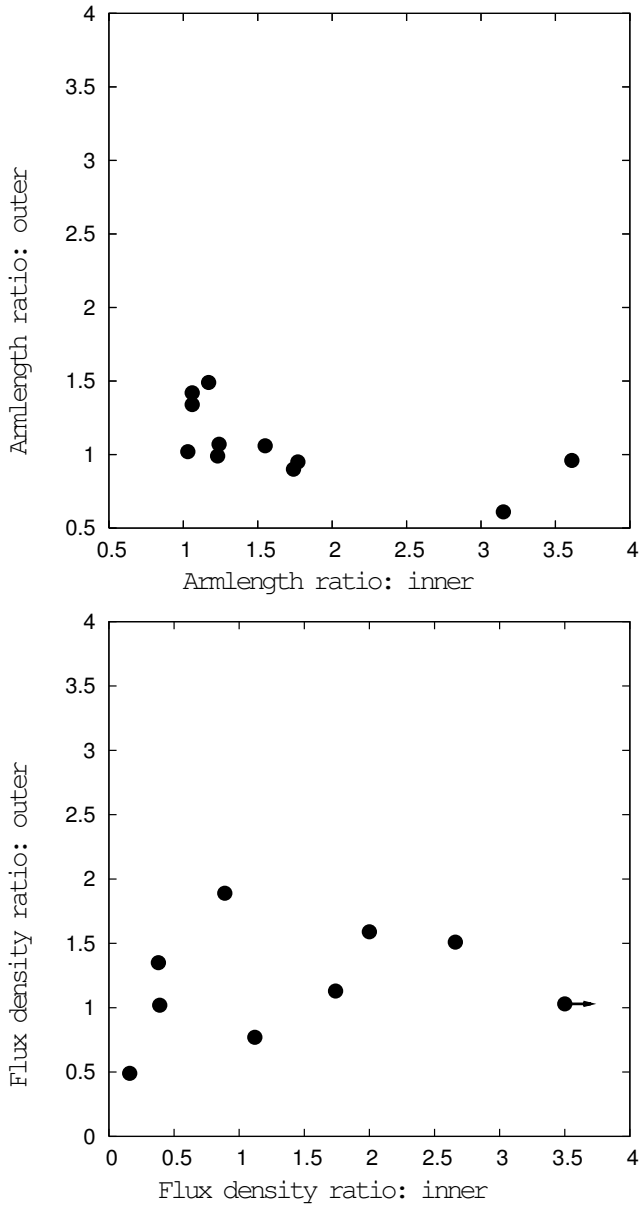

Figure 7: The armlength (upper panel) and flux density (lower panel) ratios of the inner doubles are plotted against the corresponding values for the outer doubles for the sample of DDRGs.

- **Inner double more asymmetric in its armlength ratio**
- **Inner double more asymmetric in its flux density ratio**

Symmetry parameters of DDRGs

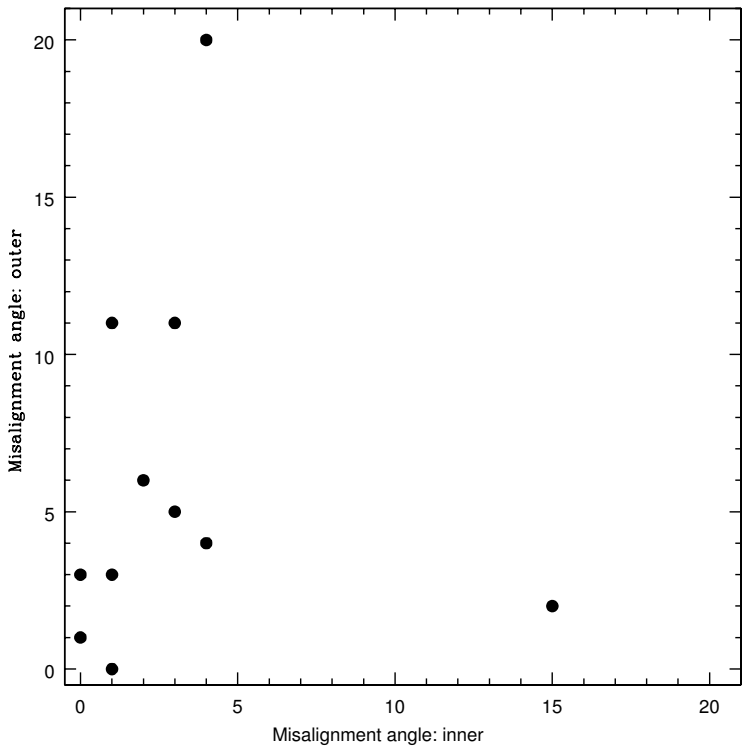

Figure 8: The misalignment angle of the outer double in degrees is plotted against the corresponding value for the inner double.

- **Inner doubles tend to be more aligned than the outer doubles.**
- **Large-scale density gradients?**
- **Motion of the parent galaxy?**

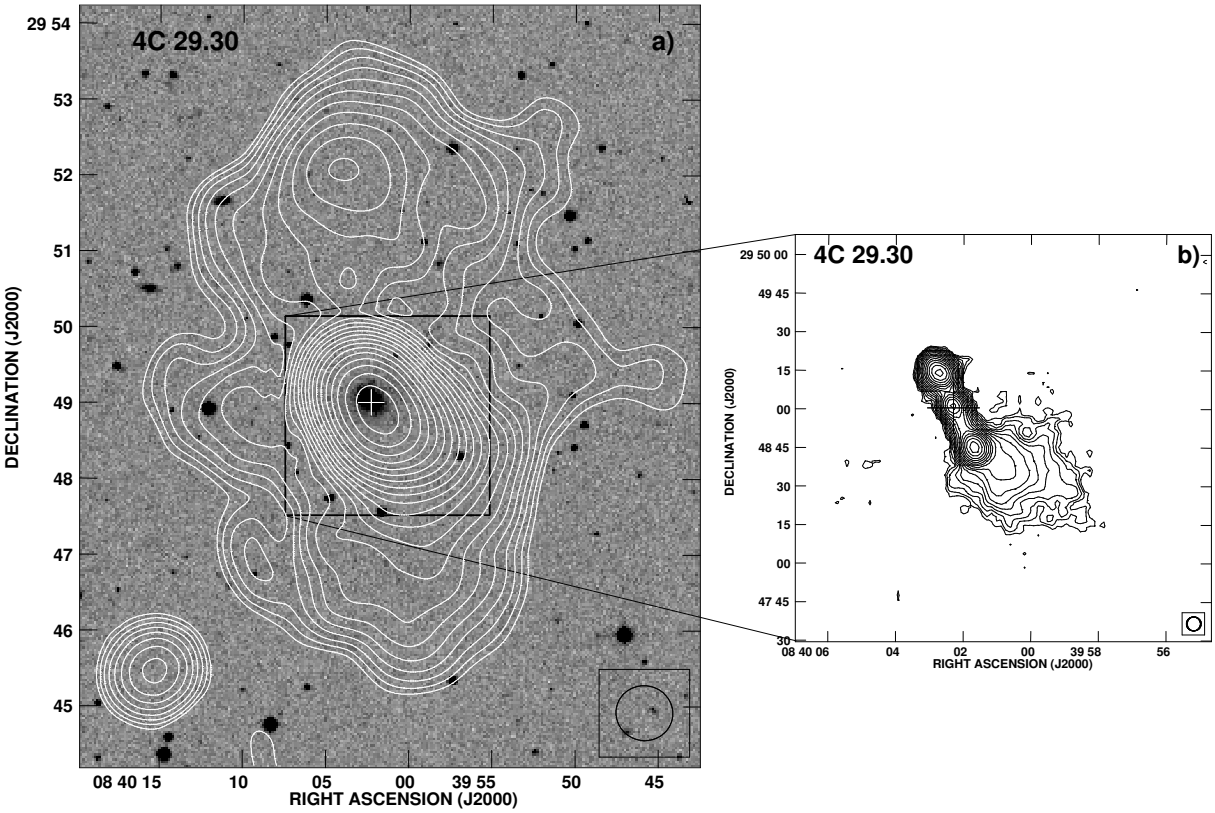

Figure 9: 1400-MHz VLA images of 4C 29.30. **a)** D-array contour map of the entire source overlayed on the optical field from the Digital Sky Survey (DSS). **b)** B-array contour map of the central part of the source from FIRST (Jamrozy, Konar, Saikia, Stawarz, Mack and Siemiginowska).

- **Outer size: 637 kpc; inner size: 36 kpc (redshift = 0.06471)**
- **Outer luminosity: $\sim 1.9 \times 10^{24}$ W Hz^{-1} at 1400 MHz; inner luminosity: $\sim 5.5 \times 10^{24}$ W Hz^{-1} at 1400 MHz**

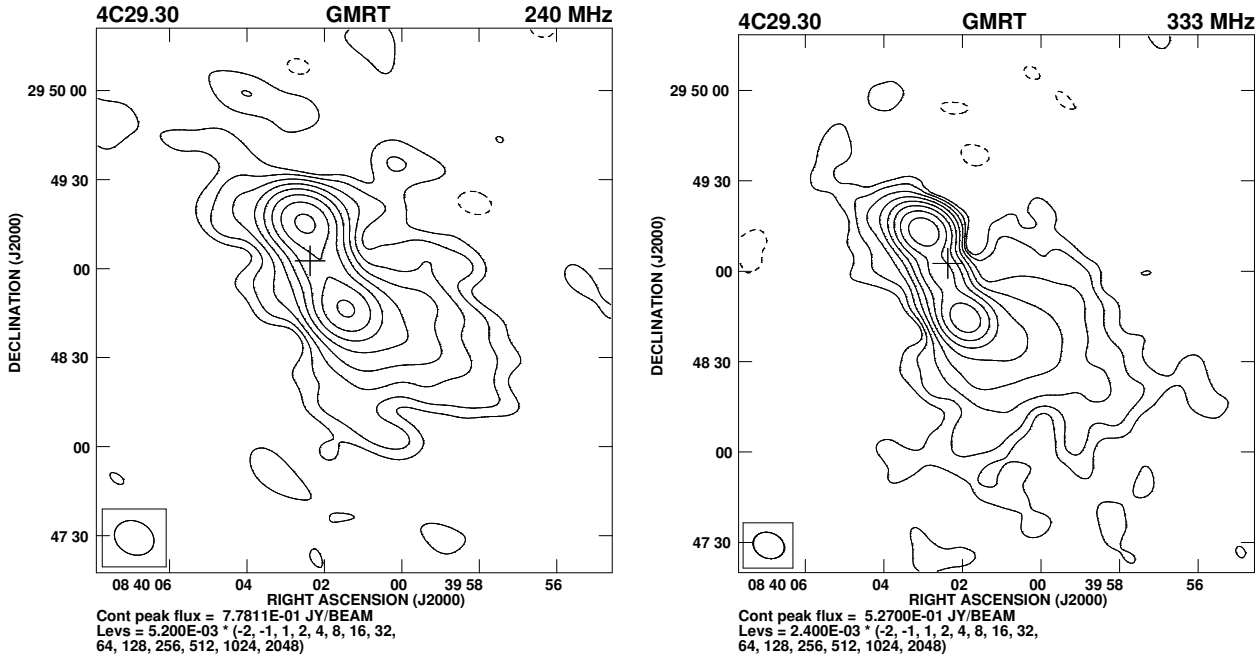

Figure 10: The GMRT images of 4C29.30. Left panel: Image at 240 MHz with an angular an angular resolution of 13.8×11.1 arcsec^2 along PA 64°; right panel: the 334-MHz image with an angular resolution of 10.6×8.5 arcsec^2 along PA 68°.

- **Spectrum of inner double determined over a large frequency range from low-frequency GMRT and higher frequency VLA observations**

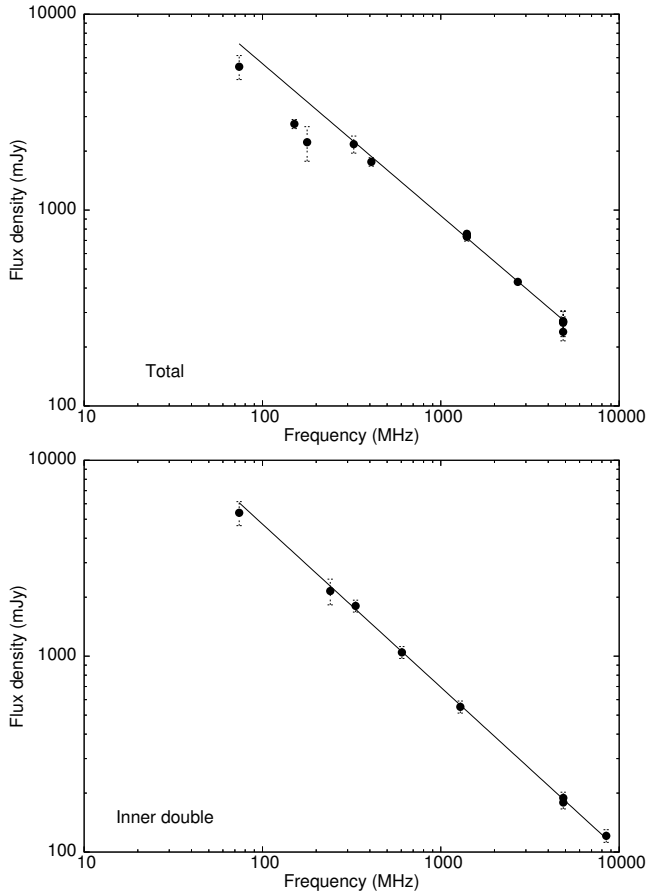

Figure 11: Upper panel: Spectrum of the 4C29.30 using flux densities from the literature. The linear least-squares fit has been made using only measurements between 325 and 4850 MHz. Lower panel: Spectrum of the inner double using our GMRT and VLA images between 235 and 8460 MHz. The contributions of the core component within a region of ∼4 arcsec (4.9 kpc) have been subtracted. The spectrum also shows the low-frequency measurement at 74 MHz from VLSS. The linear least squares fit has been made using only measurements between 235 and 8460 MHz and has been extrapolated to lower frequencies.

- **Flux densities from literature with different resolutions and sensitivities**
- **Total spectrum dominated by the inner double**
- **Spectrum of inner double determined from GMRT and VLA observations consistent with VLSS flux density**
- **Inner double is consistent with a straight spectrum**

Inermittent jet activity in the radio galaxy 4C29.30?

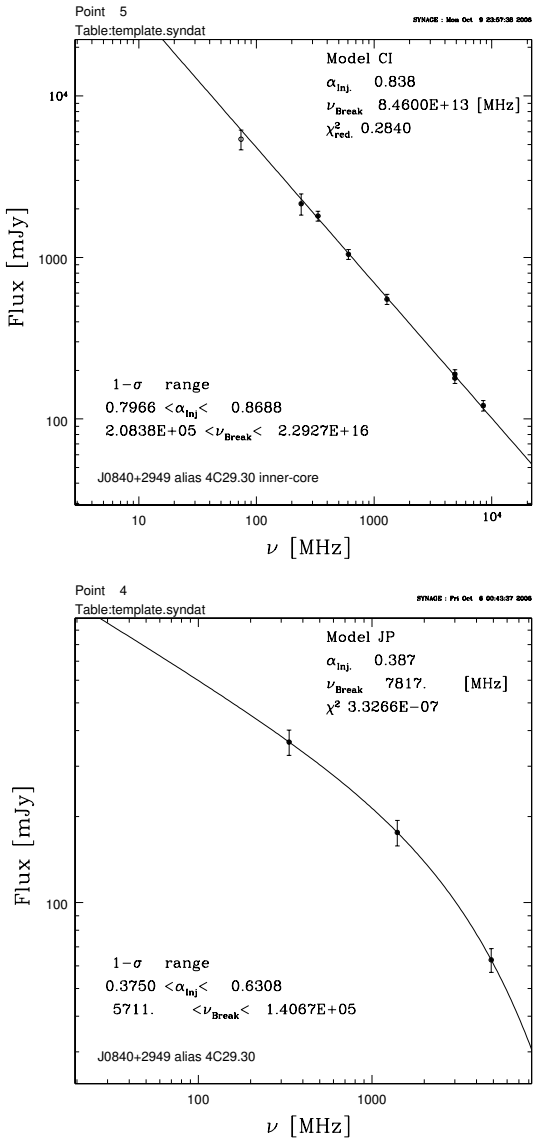

Figure 12: The radio spectrum of the inner double and a fit to it using the continuous injection model (upper panel); the radio spectrum of the diffuse emission and a fit using the Jaffe-Perola model (lower panel).

- **Inner double is consistent with a straight spectrum Estimated age is less than about 0.1 Myr**
- **Break frequency of outer emission: ∼4 to 8 GHz Estimated age is ∼34 to 47 Myr**
- **Variable core**

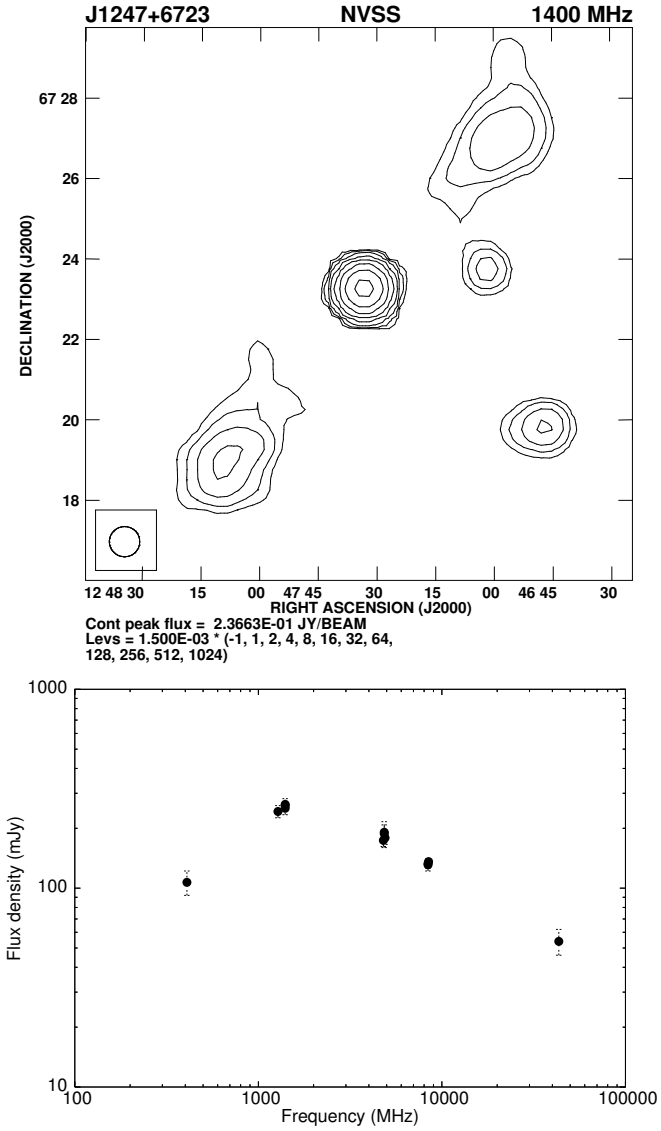

Figure 13: The NVSS image of J1247+6723 with an angular resolution of 45 arcsec (upper panel) and the radio spectrum of the central component.

- **Outer size: 1195 kpc; inner size: 0.014 kpc (redshift = 0.1073)**
- **Central component: mini double with a GPS spectrum**
- **Outer luminosity: $\sim 3.5 \times 10^{24}$ W Hz^{-1} at 1400 MHz; inner luminosity: $\sim 7.4 \times 10^{24}$ W Hz^{-1} at 1400 MHz**

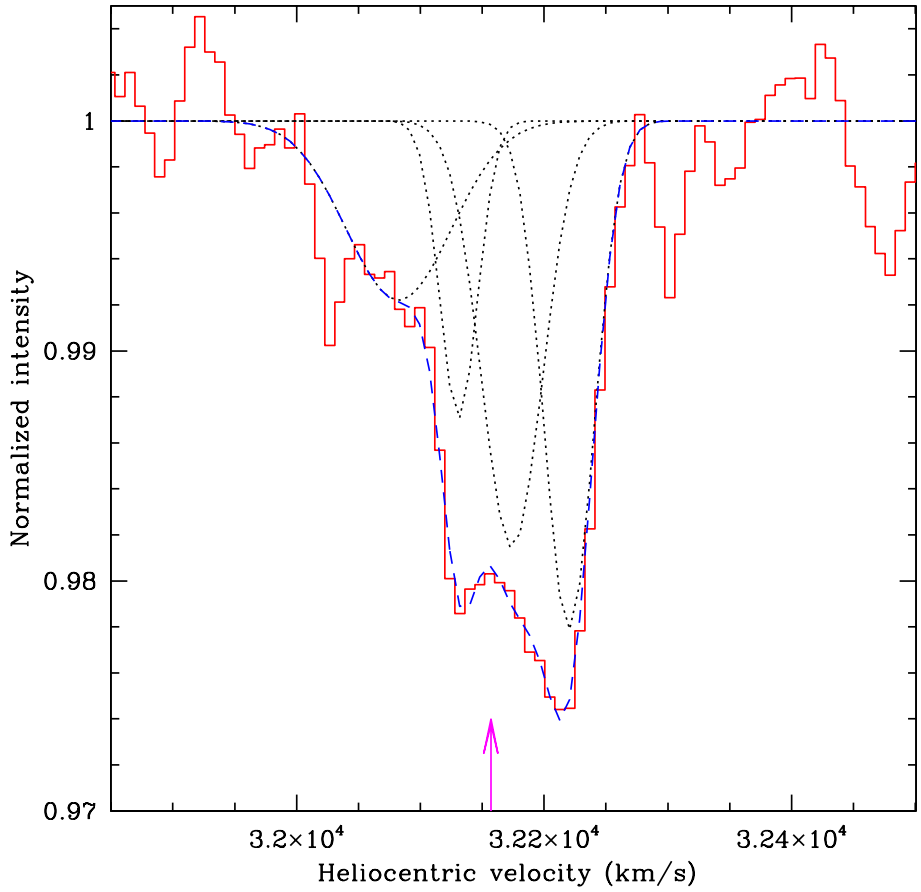

Figure 14: The HI absorption spectrum (histogram) towards the compact inner double of the radio galaxy J1247+6723. The spectrum has been smoothed using a 3-pixel wide boxcar filter. The Gaussian components fitted to the absorption profile and the sum of these components i.e. the fit are plotted as dotted and dashed lines respectively. The systemic velocity (32157 km s^{-1}) has been marked by an arrow (Saikia, Gupta and Konar 2006).

- **Absorption profile consists of four components**
- **Total HI column density is N(HI)=6.73×10^{20}(T_s/100)(f_c/1.0)$^{-1}$ cm^{-2}**
- **Close relationship between HI absorption and evidence of renewed activity**
- **Other cases: 3C236, 3C293, 3C258**